Catalytic performances of Ni–CaO–mayenite in CO_2 sorption enhanced steam methane reforming

Moisés R. Cesário [a,b], Braúlio S. Barros [c], Claire Courson [a,*], Dulce M.A. Melo [b], Alain Kiennemann [a]

[a] Institut de Chimie et Procédés pour l'Energie, l'Environnement et la Santé (ICPEES)—UMR CNRS 7515, University of Strasbourg, 67087 Strasbourg, France
[b] Department of Chemistry, Federal University of Rio Grande do Norte, 59072-970, Natal, Brazil
[c] School of Science and Technology, Federal University of Rio Grande do Norte, 59078-970 Natal, Brazil

ARTICLE INFO

ABSTRACT

Ni–CaO–mayenite ($Ca_{12}Al_{14}O_{33}$) catalysts for the CO_2 Sorption Enhanced Steam Methane Reforming (SE-SMR) have been developed using the microwave assisted self-combustion method of preparation. The sorption of CO_2 by CaO shifts the steam reforming and the Water Gas Shift reaction (WGS) towards H_2 production and favors the heat balance of the global reaction.
The CO_2 sorption has been studied on materials with different $CaO/Ca_{12}Al_{14}O_{33}$ ratios and for different types of preparation. The specific surface area of materials, the temperature of Ni phases' reducibility and CO_2 sorption are all essential for material efficiency. The Ni–CA75MM catalyst was the most active and stable in methane steam reforming with CO_2 sorption, even at an unusually low temperature (650 °C).

1. Introduction

The research and development of new sources of "clean" energy which reduce the emission of greenhouse gases are necessary. Carbon dioxide emission (CO_2) is a major contributor to global warming and one-third of those emissions come from fuel combustion for power generation [1].

Hydrogen is mainly obtained from syngas resulting from natural gas steam reforming (SMR). Syngas production by methane reforming is always accompanied by CO_2 formation, and its capture by absorption on a solid oxide could be a convenient strategy to improve CH_4 conversion and H_2 selectivity and to concentrate CO_2 for the eventual use as chemicals or as energy vectors. CaO is often chosen as the CO_2 sorbent because of its high efficiency in carbonation and its easy regeneration by $CaCO_3$ calcination. When CO_2 sorption is desired, the presence of solid oxide requires the need to work at relatively low temperatures (600–700 °C) compared to temperatures usually used in steam reforming of methane (>800 °C) [2–6]. The main reactions involved in CO_2 sorption enhanced steam methane reforming are the following:

$$CH_4 + H_2O \longleftrightarrow CO + 3H_2 \quad \Delta H_{298\ K} = 206.2\ kJ/mol \qquad (1)$$

$$CO + H_2O \longleftrightarrow CO_2 + H_2 \quad \Delta H_{298\ K} = -41.2\ kJ/mol \qquad (2)$$

$$CaO + CO_2 \longleftrightarrow CaCO_3 \quad \Delta H_{298\ K} = -178\ kJ/kmol \qquad (3)$$
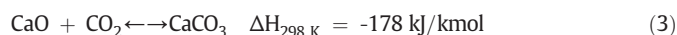
The reaction (1) is highly endothermic and thermodynamically favored by high temperature and low pressure and the Water-Gas Shift (WGS) reaction (2) is favored at low temperature and has no pressure dependence. Due to the overall endothermic nature of the reaction (1), SMR needs the occurrence of the WGS reaction. Internal carbon dioxide removal by sorption on a solid would add extra heat to the reforming reaction. An optimal temperature window for CO_2 sorption is 600–700 °C [7,8]. That could be of interest if $CaCO_3$ regeneration is performed in a second reactor together with the elimination of deposited carbon produced during the hydrocarbon reforming. The use of a sorbent in the process may lead to a high hydrogen yield. In fact, the capture of CO_2 shifts the balance towards a more favorable thermodynamic pathway for the production of pure hydrogen.

Several studies [3,9–12] indicate that the CaO-based materials have been highlighted as the solid sorbents in the capture of CO_2 because of their favorable thermodynamic and chemical properties. The main problem with CaO is the strong decrease in the sorption capacity after multiple carbonation–calcination cycles. Sintering is indicated as the cause of the referred decay [10,13,14]. Another cause can be related to the formation of a non-porous calcium carbonate layer on the CaO grain's surface. This phenomenon limits the diffusion of CO_2 to the bulk of the grain. Thus, the exothermic reaction of carbonation can be characterized by two steps: an initial step of CO_2 sorption controlled by kinetics which is followed by a slower second step controlled by CO_2 diffusion in CaO and $CaCO_3$ [15].

Several strategies are reported in the literature to prevent the decrease in sorbent efficiency due to sorption cycles and diffusion effects: optimization of calcination conditions [16,17], hydration of the sorbent [18] or deposition of calcium oxide on an inert support [4,19]. Thus, $CaAl_2O_4$ [20,21], $Ca_2Fe_2O_5$ [22] or $Ca_{12}Al_{14}O_{33}$ (mayenite) [4,23,24] have been tested for CO_2 sorption with CaO excess. $Ca_{12}Al_{14}O_{33}$ has no CO_2 sorption property but presents a large surface area and provides stable network inhibiting deactivation of CaO by sintering. $Ca_{12}Al_{14}O_{33}$ appears to be an appropriate candidate to support CaO. The properties (surface area, pore volume) of these materials are strongly dependent on the synthesis method. Previous work describes the synthesis by hydration and calcination processes [9], coprecipitation [25], mixed-precipitation [26], mechanical mixing [27,28] and sol–gel process [29]. Nickel, the metal generally used in steam reforming, can be added to the sorbent $CaO–Ca_{12}Al_{14}O_{33}$ for hydrocarbon reforming and CO_2 sorption [30].

The present work proposes a new method for the preparation of $CaO–Ca_{12}Al_{14}O_{33}$ supports with different Ca/Al ratios by microwave assisted self-combustion. This is a low cost, time-saving method with efficient preparation [31]. Then, Ni–CaO–mayenite bi-functional materials (catalysts and sorbents) for CO_2 sorption enhanced steam methane reforming were prepared by wet impregnation of Ni on the sorbent prepared by microwave assisted self-combustion. These bi-functional materials were tested in SMR at a low temperature (650 °C) and H_2O/CH_4 ratio of 3 with CO_2 capture (SE-SMR). Some studies in WGS reaction are performed after SE-SMR to prove the efficiency of the catalysts for this reaction.

2. Experimental

2.1. Sorbent preparation

The samples with CaO to $Ca_{12}Al_{14}O_{33}$ weight ratios of 75/25 and 90/10 (CA75MM and CA90MM) were prepared employing a microwave assisted self-combustion method (MM) using urea excess in the presence of ammonium nitrate. The precursors were aluminum nitrate [$Al(NO_3)_3 \cdot 9H_2O$—Merck], calcium nitrate [$Ca(NO_3)_2 \cdot 4H_2O$—Merck], urea [$CO(NH_2)_2$—Merck], and ammonium nitrate [NH_4NO_3—Merck]. Nitrates were chosen for synthesis because of their water solubility, low fusion temperature, and low cost. Urea has the advantage of being commercially available. It is relatively inexpensive and offers high heat generation which is important for the crystallization of the desired phases. The ammonium nitrate ensures reaction uniformity allowing all the reactants to decompose at the same time. The MM method could be of interest from an economical point of view (short preparation time, energy gains) but implies the development of an appropriate microwaves furnace for the preparation at an industrial scale.

Employing a microwave assisted self-combustion method, the aluminum, calcium and ammonium nitrates, also called oxidants, were mixed in a Becker type Pyrex with the reducing agent (urea), also known as fuel. After 10 min of stirring on a heating plate to 70 °C, the aqueous suspension was placed in a conventional microwave oven with an output power of 800 W and a frequency of 2.45 GHz until spontaneous ignition. The resulting powder was calcined at 900 °C for 1.5 h with a heating rate of 10 °C min^{-1} then sieved at around 100 μm.

As an example, the CA75MM sorbent (75%CaO–25%$Ca_{12}Al_{14}O_{33}$) was prepared as follows: 1.56×10^{-2} mol of calcium nitrate, 2.60×10^{-3} mol of aluminum nitrate, 6.50×10^{-3} mol of urea and 1.25×10^{-1} mol of ammonium nitrate were mixed in order to prepare 10 g of the proposed material.

Sorbents were also prepared using a natural precursor (Calcite) and aluminum nitrate (LM method) [9]. This method uses calcination and hydration processes. The natural calcite ($CaCO_3$), ARMIL Mineração do Nordeste—Brazil, was used as the calcium oxide (CaO) precursor and submitted to calcination at 900 °C for 2 h. 7.11 g of aluminum nitrate nonahydrate ($Al(NO_3)_3 \cdot 9H_2O$,—>98.0% ALFA AESAR) and 6.55 g or 17.8 g of powdered calcium oxide were added to a mixture of 2-propanol (32.5 mL or 38.6 mL) and distilled water (190 mL) so that the weight ratios of calcium oxide to newly formed materials ($Ca_{12}Al_{14}O_{33}$) would become 75/25 or 90/10 wt.%. This solution was stirred for 1 h at 75 °C and dried at 120 °C for another 18 h before calcination at 500 °C for 3 h. By this method, 2-propanol, water, and nitric acid (formed in the solution) were evaporated at different stages, thereby offering the production of fine and porous powder. Distilled water was added to the resulting powder to form a paste which was then dried at 120 °C for 2 h and calcined at 900 °C for 1.5 h with a heating rate of 10 °C min^{-1}. The obtained powders (CA75LM and CA90LM) were sieved at around 100 μm.

2.2. Catalyst preparation

The metal (Ni) impregnation was carried out with a nickel nitrate (>97% Sigma Aldrich) aqueous solution (0.62 g of salt leads to 5%wt. of Ni in relation to the final weight of the samples) on CA75MM, CA75LM, CA90MM and CA90LM sorbents. The suspension of these sorbents (2.5 g) in the nitrate nickel solution was kept under stirring at 110 °C during 30 min to induce the evaporation of the solvent, then the solid was collected, dried overnight at 100 °C and then calcined at 750 °C for 4 h, with a heating rate of 3 °C min^{-1}.

For the comparison of the sorption capacity, a sample of Ni–CaO was prepared by calcination of calcite at 900 °C for 2 h and then impregnation with 5%wt. Ni (nitrate solution) and further calcination at 750 °C for 4 h with a heating rate of 3 °C min^{-1}.

Table 1
Nomenclature and synthesis conditions adopted for each prepared sample.

Samples—composition	Precursors	Synthesis conditions	Calcination	Nomenclature
75%CaO–25%$Ca_{12}Al_{14}O_{33}$ or 90%CaO–10%$Ca_{12}Al_{14}O_{33}$	Al, Ca nitrates	Precursors in the presence of fuel (urea)[a]	RT to 900 °C/1.5 h 10 °C·min^{-1}	CA75MM or CA90MM
75%CaO–25%$Ca_{12}Al_{14}O_{33}$ or 90%CaO–10%$Ca_{12}Al_{14}O_{33}$	Al nitrate and calcined calcite	Mixing of the precursors in water and propanol, heating then drying[b]	RT to 900 °C/1.5 h 10 °C·min^{-1}	CA75LM or CA90LM
5%Ni–CaO	Calcined calcite and Ni nitrate	Ni impregnation of CaO then drying	RT to 750 °C/4.0 h 3 °C·min^{-1}	Ni–CaO
5%Ni–CA75MM or 5%Ni–CA90MM	Ni, Al, Ca nitrates	Ni impregnation of CA75MM and CA90MM then drying	RT to 750 °C/4.0 h 3 °C·min^{-1}	Ni–CA75MM or Ni–CA90MM
5%Ni–CA75LM or 5%Ni–CA90LM	Ni, Al nitrates and calcined calcite	Ni impregnation of CA75LM and CA90LM then drying	RT to 750 °C/4.0 h 3 °C·min^{-1}	Ni–CA75LM or Ni–CA90LM

RT: room temperature; x% = x wt.%.
[a] Microwave assisted self-combustion method (MM synthesis).
[b] Method based on the literature (LM synthesis).

Table 1 shows the nomenclature of the prepared samples as well as the conditions for the synthesis.

2.3. Catalysts' characterization

The catalysts were characterized by X-ray diffraction (XRD) using a Bruker D8-Advance diffractometer (Cu Kα radiation, with 40 kV and 30 mA). The diffraction powder patterns were obtained in the angular range of 10–90° using step-scanning mode (0.02°/step) with a counting time of 2 s/step. The average crystallite size of metallic nickel and calcium oxide was calculated from the broadening of the main diffraction rays using the Scherrer equation for the catalysts which underwent a reduction or the reactivity test.

The nitrogen adsorption isotherms allow the determination of specific surface area by means of the BET method (Brunauer, Emmett and Teller) on a Micrometrics Tri Star 3000 surface area analyzer. The catalysts were degassed overnight at 250 °C before being analyzed.

Temperature-programmed reduction (TPR) was carried out on a Micrometrics AutoChem II to study the reducibility of the catalysts. A mass of 50 mg was placed in a quartz U-tube (6.6 mm internal diameter) and submitted at a total gas flow of 50 mL min^{-1}, consisting of a mixture of 90% argon and 10% hydrogen. The heating rate, from room temperature to 900 °C, was 15 °C min^{-1}. A thermal conductivity detector (TCD) permitted the quantitative determination of hydrogen consumption.

2.4. Catalytic tests and ability to capture CO_2

A TGA Q500 thermal gravimetric analysis equipment was used for the carbonation and calcination experiments. 5–10 mg of catalyst was placed in a platinum/rhodium sample cup and heated at 800 °C under helium flow (10 mL min^{-1}) for 10 min to remove adsorbed water and CO_2. Then, the temperature was decreased to 650 °C and the gas mixture was changed to a 5 mL min^{-1} CO_2 flow (10% in He). The sorption duration was 30 min, following by desorption at 800 °C for 10 min under a 10 mL min^{-1} pure He flow. Multiple cycles, consisting of sorption and desorption steps, were repeated to test the ability of sorbents to keep their CO_2 sorption capacity.

The experiments of SE-SMR were carried out at 650 °C during 15 h. The operating conditions for cyclic stepwise SE-SMR over Ni/CaO–$Ca_{12}Al_{14}O_{33}$ were as follows (feed flow rates under normal conditions):

Condition 1: Ar = 26 mL min^{-1} g$_{cat}^{-1}$, CH_4 = 1.0 mL min^{-1} g$_{cat}^{-1}$ and H_2O = 3.0 mL min^{-1} g$_{cat}^{-1}$ (H_2O/CH_4 = 3), 1.0 g of catalyst (ratio of

Table 2
Specific surface area of sorbents and catalysts prepared by different methods and Ni content of catalysts.

Samples	BET surface area before reforming reaction ($\pm$ 0.1 m^{2}g^{-1})	Ni content (weight %)
CA75MM	1.2	–
CA90MM	1.3	–
CA75LM	8.2	–
CA90LM	9.2	–
Ni–CA75MM	11.5	3.6
Ni–CA90MM	6.4	3.9
Ni–CA75LM	12.6	3.6
Ni–CA90LM	8.5	4.0

sorbent to methane equal to 0.75 g min mL^{-1} and 0.90 g min mL^{-1} for 75% and 90% CaO, respectively).

Condition 2: Ar = 26 mL min^{-1} g$_{cat}^{-1}$, CH_4 = 1.0 mL min^{-1} g$_{cat}^{-1}$ and H_2O = 3.0 mL min^{-1} g$_{cat}^{-1}$ (H_2O/CH_4 = 3), 2.5 g of catalyst (ratio of sorbent to methane equal to 1.88 g min mL^{-1} and 2.25 g min mL^{-1} for 75% and 90% CaO, respectively).

Water was injected using a syringe pump. The outlet gas was analyzed by means of gas micro-chromatography apparatus equipped with two modules: (1) using a molecular sieve column for the separation of CH_4, H_2 and CO and (2) using a HayeSep column for the separation of CH_4 and CO_2. Before the reaction test, the materials were reduced in a 30%H_2/Ar flow at 800 °C for 1 h at a constant heating rate of 10 °C min^{-1}. The flow rate of H_2 was then cut and the temperature decreased to 650 °C to add water and CH_4 in a ratio of 3.

For the study of Water Gas Shift reaction, the CH_4 flow was substituted by a CO flow (H_2O/CO ratio of 1) after 20 h of SE-SMR tests.

In all the experiments, catalytic performances were evaluated by CH_4 conversion and H_2, CO, CO_2, and CH_4 molar fractions were calculated as follows:

$$\text{Conversion}(CH_4)(\%) = \frac{(CH_4)_{in} - (CH_4)_{out}}{(CH_4)_{in}} \cdot 100 \qquad (4)$$

$$\text{Molar Fraction } X_n = \frac{(AX_n \cdot f_n)}{(AX_1 \cdot f_1) + (AX_2 \cdot f_2) + (AX_3 \cdot f_3) + (AX_4 \cdot f_4)} \qquad (5)$$

X: product; A: peak area; f: response factor and n: variation 1–4 for the four compounds (H_2, CO, CO_2, CH_4).
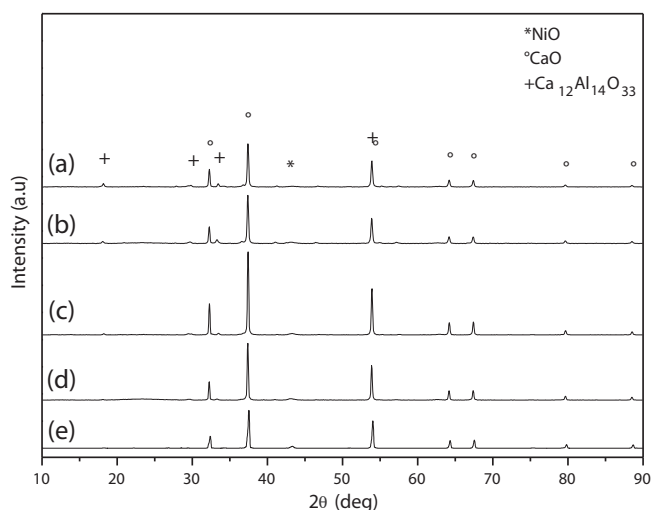
Fig. 1. XRD patterns of samples: (a) Ni–CA75MM, (b) Ni–CA75LM, (c) Ni–CA90MM, (d) Ni–CA90LM and (e) Ni–CaO.
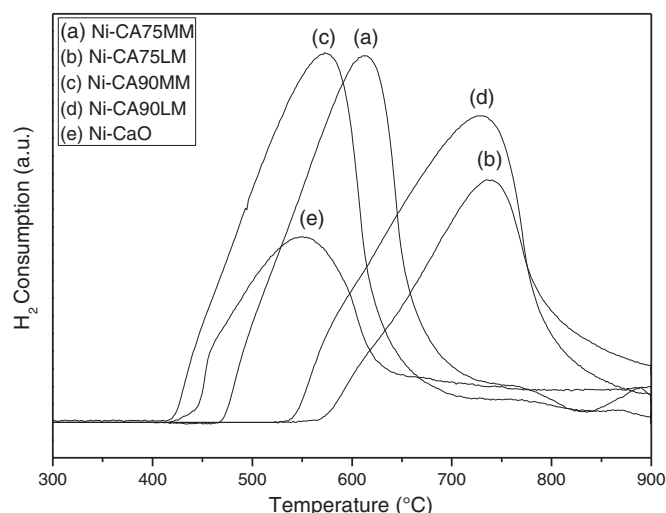
Fig. 2. Temperature-programmed reduction (TPR) profiles of the catalysts.

Table 3
Ni crystallite size of the catalysts prepared by different methods after reduction.

Samples	Crystallite size after reduction (nm)
Ni–CA75MM	22.3
Ni–CA90MM	20.5
Ni–CA75LM	19.4
Ni–CA90LM	20.5

3. Results and discussion

3.1. Characterization of sorbents and catalysts

3.1.1. XRD

X-ray diffraction patterns of the catalysts (Ni–CA75MM, Ni–CA75LM, Ni–CA90MM, Ni–CA90LM and NiO–CaO) are shown in Fig. 1.

The structure phases of NiO (JCPDS File No. 73-1519, with space group Fm-3m, $2\theta = 43,39°$), CaO (JCPDS File No. 78-0649, with space group Fm-3m) and $Ca_{12}Al_{14}O_{33}$ (JCPDS File No. 48-1882, with space group I-43d) were observed. For a comparison, a standard (Ni–CaO) was prepared. According to Fig. 1, no formation of solid solution between NiO and CaO nor $NiAl_2O_4$ spinel phase was detected. NiO and CaO phases were easily detected.

Preparation methods and calcination conditions ensure the selective formation of $Ca_{12}Al_{14}O_{33}$. No diffraction ray corresponding to another Ca–Al phase such as $Ca_3Al_2O_6$, $CaAl_2O_4$, $CaAl_4O_6$ or $CaAl_{12}O_{19}$ was observed. After Ni nitrate impregnation and calcination, neither spinel-type ($NiAl_2O_4$) nor hydrated structures $Ca(OH)_2$ were identified, irrespective of the preparation method used. The absence of those crystalline phases in the catalysts is important for both the CO_2 sorption and the steam methane reforming activity [32].

3.1.2. BET

Table 2 shows the sorbents and catalysts surface area.

The surface areas of the LM sorbents (CA75LM and CA90LM) are higher than those of MM sorbents (CA75MM and CA90MM) due to the hydration stage used in the preparation. Previous studies [18] report that the addition of water in the preparation stage of the sorbents may be responsible for producing regular hexagonal crystalloid $Ca(OH)_2$ which becomes porous CaO during calcination at 900 °C and leads to an increase in surface area.

Such phenomenon also occurs during the impregnation of the support with Ni salt. Thus, surface area values of the catalysts prepared via wet impregnation of the support (MM and LM methods) are significantly higher than the sorbents surface prepared employing the MM method. The difference of the BET surface between Ni–CA75LM and Ni–CA90LM and between Ni–CA75MM and Ni–CA90MM is due to the amount of CaO present in the samples.

Irrespective of the preparation method, the surface areas of the catalysts are similar (Ni–CA75MM and Ni–CA75LM or Ni–CA90MM and Ni–CA90LM) within experimental error even if the initial surface areas of the supports are different. This is due to the support impregnation by a Ni salt aqueous solution for the MM catalysts and, as indicated before, to the production of porous CaO after calcination.

3.1.3. TPR

The TPR profiles of Ni catalysts are shown in Fig. 2.

The TPR profiles of the catalysts prepared by impregnation of the sorbents with an excess of CaO obtained by MM are shown in Fig. 2 (curves a and c). The maximum reduction peak is between 560 and 620 °C. A slight shoulder appears between 420 and 500 °C which can be considered as the result of the reduction of free NiO. At high temperature (750–800 °C) a small reduction peak, probably assigned to the spinel-like structure $NiAl_2O_4$, can be observed (not seen by XRD). This phase may have been formed during preparation or during TPR. The first and last signals are always of low intensity. The main signal is larger and corresponds to the reduction of nickel in strong interactions with CaO and $Ca_{12}Al_{14}O_{33}$. It can be noticed that higher CaO excess gives the lowest reduction peak temperature (560 compared to 620 °C). This implies that NiO–$Ca_{12}Al_{14}O_{33}$ inter-actions are stronger than a NiO–CaO interaction which is confirmed by the curve 2e (Ni–CaO) where the maximum of NiO reduction is located at 550 °C.

TPR profiles of LM catalysts are different (curves b and d). There is a shift of the main peak towards higher temperatures (750 °C) which indicates stronger metal–support interactions. There is no free NiO. However, there are possible Ni–Al oxide interactions. The difficulty of the reduction of the LM catalyst may have an influence on their reactivity since only a partial reduction of the sample would occur at 600–700 °C.

The diffraction patterns of catalysts after the TPR experiments (not given) show well defined diffraction rays of metallic nickel (JCPDS File No. 87-0712, with space group Fm-3m), CaO and $Ca_{12}Al_{14}O_{33}$. The average crystallite size of metallic nickel (Table 3) is about 19–23 nm for all the samples (Ni–CA75MM, Ni–CA90MM, Ni–CA75LM, Ni–CA90LM and Ni–CaO) prepared using different methods.
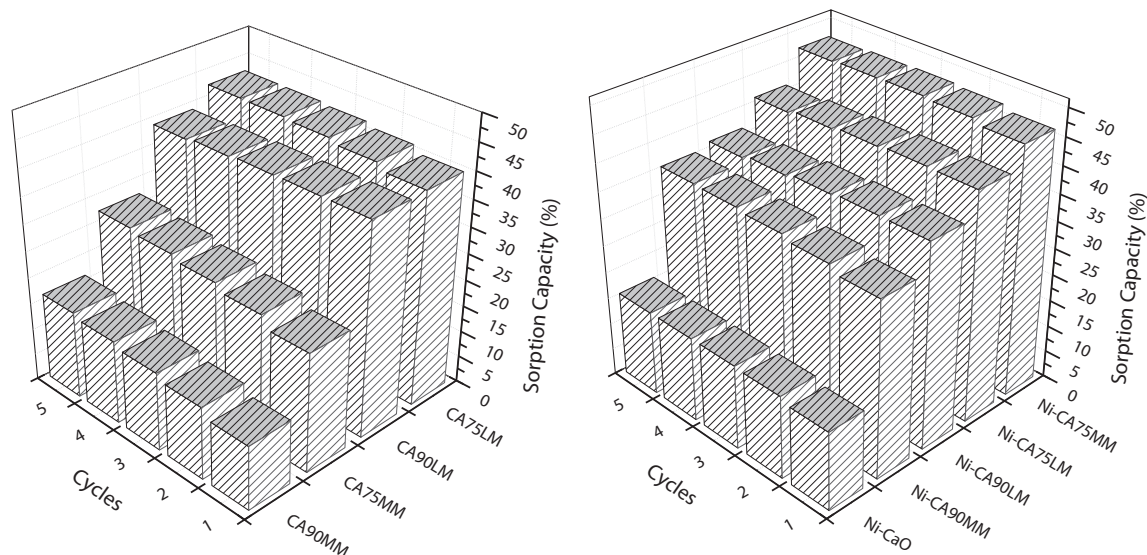
Fig. 3. Comparison of cyclic CO_2 sorption capacity on the sorbents (left) and catalysts (right) (CO_2 sorption: 650 °C, 30 min, 10% CO_2/He; desorption: 800 °C, 10 min, 100% He).
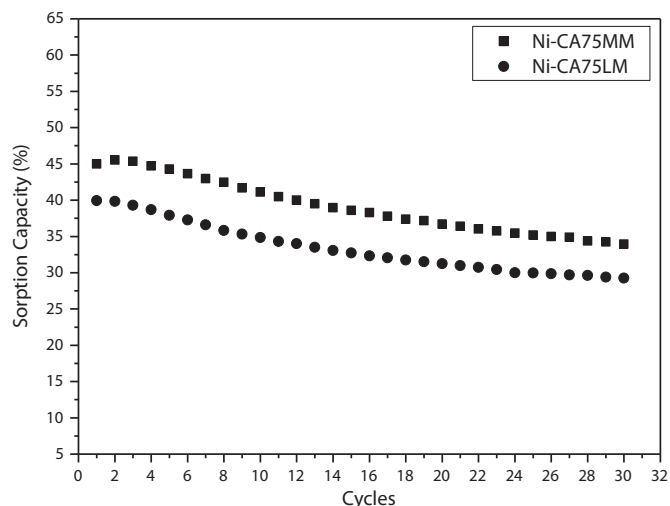
Fig. 4. CO_2 sorption capacity of Ni–CA75MM and Ni–CA75LM during 30 cycles of sorption/desorption. (CO_2 sorption: 650 °C, 30 min, 10% CO_2/He; desorption: 800 °C, 10 min, 100% He).

3.2. CO_2 sorption experimental results

Fig. 3 shows the CO_2 sorption capacity of the sorbents (left) and catalysts (right) after five carbonation/calcination cycles. The sorption capacity was defined as a fraction of the experimental amount of CaO (total carbonation) and the theoretical value of free CaO in the material.

After five sorption/calcination cycles, the CO_2 sorption capacity of the sorbents CA90MM, CA75MM, CA90LM and CA75LM reached values of 17.0, 27.0, 39.0, and 43.0%, respectively.

During the five cycles both CA75MM and CA90MM samples showed a slight increase in sorption capacity. The CA90MM sorbent exhibits a lower performance than the CA75MM sorbent due to the more important formation of a $CaCO_3$ layer which blocks the CO_2 sorption on CaO up to the heart of the grain. CA75LM and CA90LM sorbents showed higher sorption capacity than those prepared by microwaves assisted self-combustion (CA75MM and CA90MM). The hydration process linked to the preparation method had a positive effect on the surface area and, consequently, increased the sorption capacity of the LM sorbents.

After Ni impregnation, the Ni–CA90MM, Ni–CA90LM, Ni–CA75LM and Ni–CA75MM samples reached a CO_2 sorption capacity of 36.0, 36.0, 41.0 and 47.0%, respectively.

During the five cycles, the Ni–CA75MM catalyst showed a higher sorption capacity compared to catalyst with CaO excess (Ni–CA90MM) for the same reason as discussed for the CA75MM and CA90MM sorbents. The presence of Ni greatly improves the sorption properties (Ni–CA75MM and Ni–CA90MM compared to CA75MM and CA90MM, respectively). Ni–CA75MM showed a slightly higher sorption capacity than Ni–CA75LM which is contrary to lone sorbents. The sorption capacity improvement after Ni salt impregnation (Ni–CA75MM compared to CA75MM) is related to the increase in BET surface area (Table 2) and due to the hydration process. Martavaltzi et al. [33] also pointed out that the presence of NiO helped to optimize the CO_2 sorption capacity.

Irrespective of the preparation method, the presence of $Ca_{12}Al_{14}O_{33}$ enhances sorption capacity (compared to the Ni–CaO catalyst). This is in
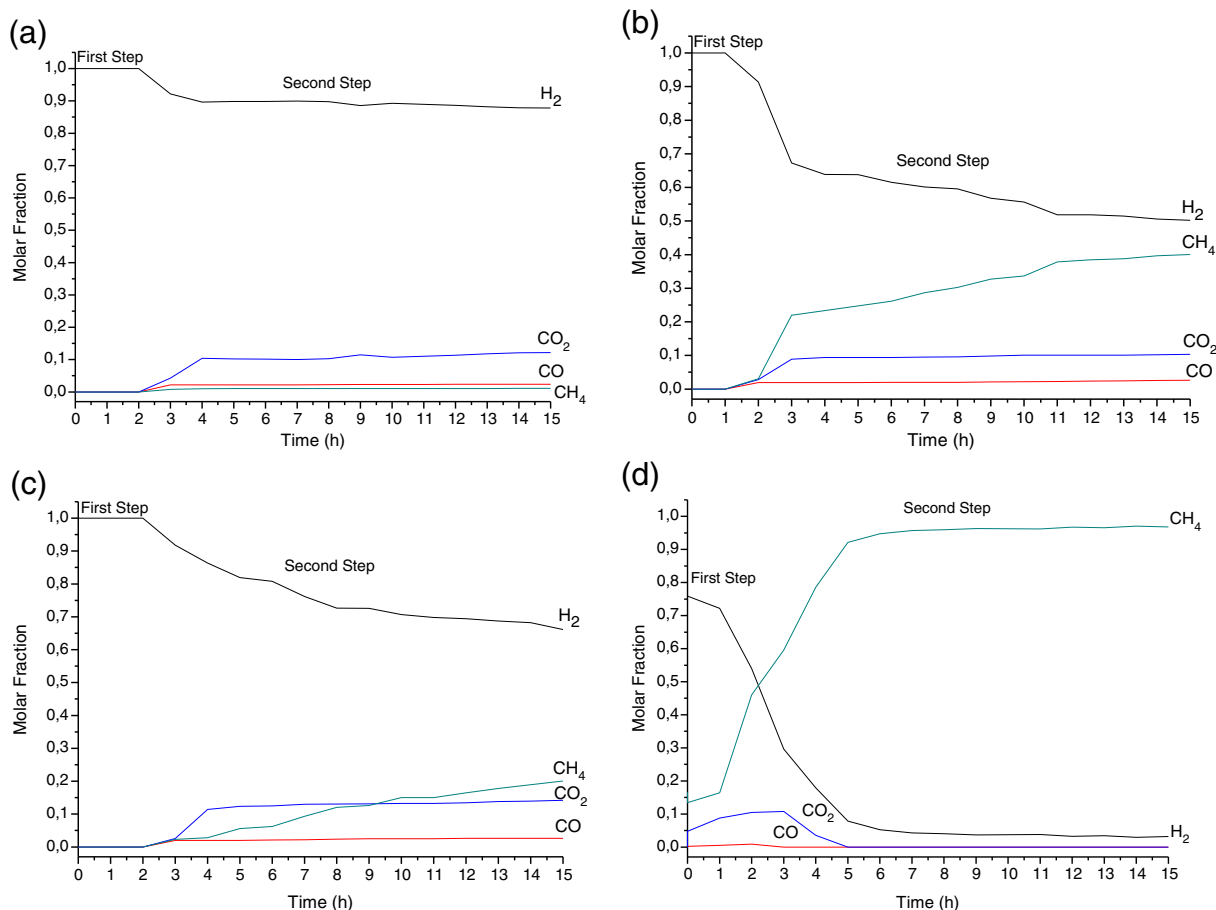
Fig. 5. CO_2 sorption enhanced steam methane reforming: molar fraction of methane and products versus time (a) Ni–CA75MM; (b) Ni–CA90MM; (c) Ni–CA75LM and (d) Ni–CaO. Reaction conditions: total flow rate = 30 mL min^{-1} (Ar = 26 mL min^{-1}, CH_4 = 1.0 mL min^{-1}, H_2O = 3.0 mL min^{-1}), mass of catalyst = 1.0 g, H_2O/CH_4 molar ratio = 3, temperature 650 °C.

accordance with a more appropriate dispersion of the calcium oxide phase between the calcium aluminate grains preventing the agglomeration of both CaO (responsible for CO_2 capture) and $CaCO_3$.

Sorption capacities of Ni–CA75MM and Ni–CA75LM were evaluated using a larger number of sorption/desorption cycles in order to verify the stability of the sorption capacity over a long period. Fig. 4 shows the performance over 30 cycles of carbonation/calcination.

A similar decay in sorption capacity was observed for the two preparation methods (MM and LM). After 24 cycles, CO_2 sorption reaches 35% and 29% for Ni–CA75MM and Ni–CA75LM, respectively, and then stabilizes. Previous studies have already shown the stability of CaO in repeated sorption–desorption cycles due to the use of $Ca_{12}Al_{14}O_{33}$ in the matrix [4,9].

3.3. Activity for sorption enhanced steam methane reforming (SE-SMR)

Fig. 5 shows the performance of the catalysts in SMR enhanced by CO_2 sorption.

The SMR enhanced by CO_2 sorption process is divided into two steps (Fig. 5), in which the total time of the first depends on the properties of the sorbent (sorption capacity and sorption kinetics) as well as the operating conditions [2].

According to Fig. 5a, the Ni–CA75MM catalyst shows a breakthrough time for CO_2 equal to 2 h (first step). In the first step, hydrogen alone is present as product in the gas phase and the conversion of CH_4 is 100%. The entire CO produced during steam reforming is oxidized into CO_2 which is completely sorbed. The activation of the three reactions of the process (reforming reaction, water gas shift and carbonation) occurs. CO_2 sorption enhances methane and CO conversion; H_2 increases which is in agreement with the hypothesis based on the shift of the equilibrium of the steam reforming and water gas reactions.

A decrease in the formation of hydrogen associated with an increase in CO, CO_2 and methane is then observed (second step). This corresponds, exactly, to the end of the CaO carbonation (confirmed by XRD). Therefore, CO_2 sorption is no longer possible, so the steam reforming and water gas shift reactions are not shifted (reactions 1 and 2). Finally, hydrogen formation and methane conversion remain constant but at a lower level.

The Ni–CA90MM catalyst (Fig. 5b) showed a breakthrough time (1 h) for CO_2 lower than the Ni–CA75MM catalyst. This can be justified by a greater sorption capacity of Ni–CA75MM. In the second step, a sudden drop in hydrogen concentration associated with an increase in CO, CO_2 and methane is observed. The Ni–CA90MM catalyst showed a weaker performance compared to the other catalysts. That can be associated with the rapid sintering of the CaO particles or with the formation of a layer of $CaCO_3$ that prevents the diffusion of CO_2 and its sorption on the available CaO. With lower CaO excess (48 and 65%), the methane conversion is similar to the catalyst containing a 75% CaO excess but the breakthrough time (curves not given) is reduced to 30 and 50 min, respectively.

The Ni–CA75LM catalyst (Fig. 5c) showed a breakthrough time for CO_2 (first step) similar to the Ni–CA75MM catalyst and similar CO_2 sorption capacity. However, after this period its activity regularly decays over time.

Fig. 5d shows the performance of the NiO–CaO catalyst. This figure clearly shows the importance of the $Ca_{12}Al_{14}O_{33}$ phase. The

Fig. 6. CO_2 sorption enhanced steam methane reforming: molar fraction of methane and products versus time (Ni–CA75MM). Reaction conditions: total flow rate = 30 mL min^{-1} (Ar = 26 mL min^{-1}, CH_4 = 1.0 mL min^{-1}, H_2O = 3.0 mL min^{-1}), mass of catalyst = 2.5 g, molar H_2O/CH_4 ratio = 3, temperature 650 °C.

agglomeration of CaO for Ni–CaO catalyst (Table 4) in relation with a strong decrease in CO_2 sorption (Fig. 3) can be the cause of the low performance of this catalyst. In fact, this catalyst is the only one where CaO particles size grows during the catalytic test.

To study the aging of the catalyst, long term catalytic tests were also performed. Fig. 6 shows the behaviour of the catalyst Ni–CA75MM during 50 h of reaction. The greatest time observed for the first step is due to the increase in the sorbent/methane ratio compared to the previous reaction conditions (2.5 times).

After the first step (saturation of CaO), hydrogen production was stable for a period of 50 h (second step) when the reaction is carried out using the catalyst obtained using the MM method. CO and CO_2 formation and methane conversion also remain constant during this time.

The after reactivity characterizations seem to point to the fact that activity decay after 7 h is probably not due to the increase in Ni particles size: about 19–23 nm after reduction (Table 3) and between 22 and 29 nm after 15 h or 50 h of reaction for all the catalysts (Table 5).

Additionally, carbon deposition after testing stays at a low level. It was calculated from the profiles of temperature programmed oxidation of the residual carbon after a temperature programmed desorption of species containing CO_2 like carbonates or hydrogencarbonate (not shown). Ni–CA75MM and Ni–CA90MM showed no carbon deposition while Ni–CA75LM showed a deposition of 3.0×10^{-4} mol carbon $g_{cat}^{-1} \times$ mole of converted CH_4^{-1} (at 600 °C). So, activity decay (between steps 1 and 2) would be due to the end of carbonation. To be sure that WGS reaction really occurs in the presence of the catalyst, the behaviour of Ni–CA75MM has been studied in this reaction (Fig. 7).

As soon as CH_4 has been cut, H_2 decreases and CO_2 increases abruptly, then stabilizes for a long period. The entire CO is consumed and the H_2/CO_2 ratio near 1 leads to the conclusion that the WGS reaction is catalyzed by these catalysts.

4. Conclusions

A new method for the preparation of Ni–CaO–mayenite bifunctional materials (catalyst/sorbent) was developed. Some synthesis

Table 4
Crystallite size of CaO before and after reaction.

Samples	Crystallite size before reaction (nm)	Crystallite size after reaction (nm)
Ni–CA75MM	31.7	30.2
Ni–CA90MM	32.3	31.5
Ni–CA75LM	31.4	30.8
Ni–CA90LM	32.6	31.7
Ni–CaO	31.1	39.7

Table 5
Ni crystallite size of the catalysts prepared by different methods after reaction.

Samples	Test duration (h)	Crystallite size after reaction (nm)
Ni–CA75MM	50	27.9
Ni–CA90MM	15	28.3
Ni–CA75LM	15	22.6
Ni–CA90LM	15	25.3
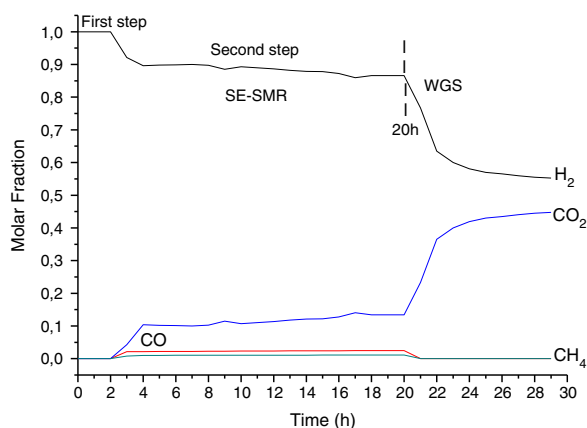
Fig. 7. CO_2 sorption enhanced steam methane reforming (SE-SMR) and Water Gas Shift reaction (WGS) with Ni–CA75MM. SE-SMR reaction conditions: total flow rate = 30 mL min^{-1} (Ar = 26 mL min^{-1}, CH_4 = 1.0 mL min^{-1}, H_2O = 3.0 mL min^{-1}), mass of catalyst = 1.0 g, H_2O/CH_4 molar ratio = 3, temperature 650 °C. WGS reaction conditions: H_2O/CO molar ratio = 1.

parameters were studied and related to the sorption properties of the materials. The hydration stage used in the MM and LM methods showed a positive effect by increasing the surface area and consequently the sorption capacity of CO_2. The presence of $Ca_{12}Al_{14}O_{33}$ enhanced the sorption capacity of the sorbents after multiple cycles of carbonation/calcination. Through the TPR profiles, it has been observed that the preparation of the catalysts obtained by wet impregnation of the sorbent (MM method) were more promising: MM catalysts were reducible at temperatures lower than the LM catalysts, which justify their higher activities. The Ni catalysts have been tested in catalytic steam methane reforming (SMR) with simultaneous sorption of CO_2. The results show that the formation of hydrogen can be optimized via steam methane reforming with simultaneous CO_2 capture using CaO dispersed on an adequate support. There is an optimal CaO/support ratio and the best compromise corresponds to an excess of 75% of CaO. The CaO carbonation shifts the equilibrium of the Water Gas Shift and improves both the productivity of SMR and the selectivity to hydrogen (100% hydrogen production). After total carbonation of the CaO, the methane conversion decreases, and CO and CO_2 appear in the gas phase. The Ni–CA75MM catalyst was the most active and stable in CO_2 sorption enhanced

steam methane reforming, even at an unusually low temperature (650 °C).

Acknowledgments

References

[1] IPCC, Climate Change 2007: Synthesis Report, in: Core Writing Team, R.K. Pachauri, A. Reisinger (Eds.), Contribution of Working Groups I, II and III to the Fourth Assessment Report of the Intergovernmental Panel on Climate Change, IPCC, Geneva, Switzerland, 2007 (104 pp.).
[2] C.S. Martavaltzi, E.P. Pampaka, E.S. Korkakaki, A.A. Lemonidou, Energy Fuel 24 (2010) 2589.
[3] L. Di Felice, C. Courson, N. Jand, K. Gallucci, P.U. Foscolo, A. Kiennemann, Chem. Eng. J. 154 (2009) 375.
[4] C.S. Martavaltzi, A.A. Lemonidou, Microporous Mesoporous Mater. 110 (2008) 119.
[5] N.H. Florin, A.T. Harris, Chem. Eng. Sci. 63 (2008) 287.
[6] K. Johnsen, H.J. Ryu, J.R. Grace, C.J. Lim, Chem. Eng. Sci. 61 (2006) 1191.
[7] D.K. Lee, I.H. Baek, W.L. Yoon, Chem. Eng. Sci. 59 (2004) 931.
[8] N. Hildenbrand, J. Readman, I.M. Dahl, R. Blom, Appl. Catal. A 303 (2006) 131.
[9] Z.-s. Li, N.-s. Cai, Y.-y. Huang, H.-j. Han, Energy Fuel 19 (2005) 1447.
[10] J.C. Abanades, D. Alvarez, Energy Fuel 17 (2003) 308.
[11] N.H. Florin, A.T. Harris, Energy Fuel 22 (2008) 2734.
[12] H. Lu, E.P. Reddy, P.G. Smirniotis, Ind. Eng. Chem. Res. 45 (2006) 3944.
[13] G.P. Curran, C.E. Fink, E. Gorin, in: F.C. Schora (Ed.), Fuel Gasification, American Chemical Society Publisher, Washington DC, 1966, p. 141.
[14] R. Barker, J. Appl. Chem. Biotechnol. 24 (1974) 221.
[15] S. Castilho, A. Kiennemann, M.F.C. Pereira, Chem. Eng. J. 226 (2013) 146.
[16] A. Silaban, D.P. Harrison, Chem. Eng. Commun. 137 (1995) 177.
[17] R.W. Hughes, D. Lu, E.J. Anthony, Y. Wu, Ind. Eng. Chem. Res. 43 (2004) 5529.
[18] C.S. Martavaltzi, A.A. Lemonidou, Ind. Eng. Chem. Res. 47 (2008) 9537.
[19] M. Broda, C.R. Müller, Adv. Mater. 24 (2012) 3059.
[20] Z.-s. Li, N.-s. Cai, Y.-y. Huang, H.-j. Han, Ind. Eng. Chem. Res. 45 (2006) 1911.
[21] Y. Li, R. Sun, C. Liu, H. Liu, C. Lu, Int. J. Greenh. Gas Control. 9 (2012) 117.
[22] L. Di Felice, C. Courson, P.U. Foscolo, A. Kiennemann, Int. J. Hydrogen Energy 36 (2011) 5296.
[23] Z. Zhou, Y. Qi, M. Xi, Z. Cheng, W. Yuan, Chem. Eng. Sci. 74 (2012) 172.
[24] J. Mastin, A. Aranda, J. Meyer, Energy Procedia 4 (2011) 1184.
[25] H. Chen, C. Zhao, Chem. Eng. J. 171 (2011) 197.
[26] N. Florin, P. Fennell, Energy Procedia 4 (2011) 830.
[27] C. Li, D. Hirabayashi, K. Suzuki, Appl. Catal. B 88 (2009) 351.
[28] V. Manovic, E.J. Anthony, Environ. Sci. Technol. 43 (2009) 7117.
[29] M. Broda, A.M. Kierzkowska, C.R. Müller, Environ. Sci. Technol. 46 (2012) 10849.
[30] M. Broda, A.M. Kierzkowska, D. Baudouin, Q. Imtiaz, C. Copéret, C.R. Müller, ACS Catal. 2 (2012) 1635.
[31] B.S. Barros, D.M.A. Melo, S. Libs, A. Kiennemann, Appl. Catal. A 378 (2010) 69.
[32] A.A. Lemonidou, I.A. Vasalos, Appl. Catal. A 228 (2002) 227.
[33] C.S. Martavaltzi, A.A. Lemonidou, Chem. Eng. Sci. 65 (2010) 4134.